
PERGAMON Mathematical and Computer Modelling 33 (2001) 1177–1202

MATHEMATICAL AND COMPUTER MODELLING

www.elsevier.nl/locate/mcm

Application of the Mixed Finite-Element Method to Rotor Blade Modal Reduction

G. C. RUZICKA
Army/NASA Rotorcraft Division
Aeroflightdynamics Directorate (AMRDEC)
U.S. Army Aviation and Missile Command, Ames Research Center
Moffett Field, CA 94035, U.S.A.
gruzicka@mail.arc.nasa.gov

D. H. HODGES
School of Aerospace Engineering. Georgia Institute of Technology
Atlanta, GA 30332, U.S.A.
dhodges@mail.ae.gatech.edu

Abstract—A mixed finite element is investigated as a means for achieving accurate modal reduction of rotor blades in finite-element software. A rationale for mixed finite elements is developed by investigating the modal reduction accuracy of a series of blade analysis methods that introduces, in a step-by-step fashion, the key features of the mixed element. During this investigation, the shortcomings of classical, displacement-based finite elements are examined qualitatively and through calculations of articulated blade response. The formal derivation of the mixed element starting from a mixed variational principle is then summarized, and finally, numerical examples are presented to demonstrate the element's modal reduction accuracy. © 2001 Elsevier Science Ltd. All rights reserved.

Keywords—Mixed finite elements, Beam theory, Rotor blades, Modal reduction.

1. INTRODUCTION

The application of the finite-element method to rotorcraft analysis over the past two decades has removed the topological restrictions on the models that can be analyzed using older, so-called "first generation" rotorcraft codes. Unfortunately, this improvement has come at a high cost: the models are appreciably larger and more costly to analyze. It is widely recognized that a key aspect to improving the efficiency of comprehensive rotorcraft analysis software is reducing the size of the computational model in a way that retains the model's essential physics. The most common means for achieving this is the *modal reduction* process, which reduces the size of the model through a basis transformation of the model's degrees of freedom. Usually, the basis transformation is a reduced set of the model's eigenmodes computed about some convenient state. Observe that this process, which involves collapsing a complex finite-element model to a smaller number of modal coordinates, is different from formulating the model's equations in modal space *ab initio*, as is done in first-generation rotorcraft codes. Unfortunately, modal

The authors are grateful for the valuable assistance provided by Professor O. Bauchau of the Georgia Institute of Technology, whose excellent study on using the mixed finite-element method for the dynamic analysis and modal reduction of rotor blades was a key motivation for this study. The authors also acknowledge the many valuable inputs they received from W. R. Johnson of the Army/NASA Rotorcraft Division at Ames Research Center.

PII: S0895-7177(00)00306-X

reduction is far from foolproof. For linear systems, the number of modes needed is a function only of the excitation, but in practice, determining the correct number can be complicated. It is usually accomplished by comparing the model's eigenvalues with the excitation's frequency content, supplemented by trial-and-error. For nonlinear systems, the process is often far more involved because the system's nonlinearity couples the eigenmodes whenever the system moves away from the state about which the basis is calculated. The set of modes needed to accurately model a nonlinear system is therefore a complex function of the excitation amplitude, as well as the frequency content, and many modes—sometimes an unfeasibly large number—may be needed to achieve reasonable accuracy if the system is highly nonlinear.

The application of modal reduction to rotor blades is problematic owing to the *centrifugal stiffening effect*, which is the geometric stiffness generated by the axial forces that arise from the blade's spin. Indeed, the effect of this geometric stiffness, say on the natural frequencies of the rotating blade, is typically far greater than that of the bending stiffness. Thus, it is crucial that a blade analysis scheme be able to represent this phenomenon accurately. However, the accuracy with which blade eigenmodes approximate centrifugal stiffening—hence, blade response—hinges critically on how the blade equations are formulated. Several formulations have been proposed in the rotorcraft literature and elsewhere to deal with this problem. The oldest and most widely used approach involves parameterizing the axial displacement using the non-Lagrangian *axial elongation* variable instead of the *axial displacement* variable, and was proposed independently by Smith [1] and by Kane *et al.* [2]. The effectiveness of the approach has been well documented, but the non-Lagrangian nature of the variable complicates the finite-element assembly process, a feature which has spurred the search for alternative approaches. Shaw and Pierre [3] have proposed a *nonlinear mode* concept, which is intriguing because it potentially can be applied to any mechanical nonlinearity, but although it has often been shown to be effective, its implementation is quite involved. Mixed finite elements, hereafter abbreviated as "mixed elements", have been proposed for rotor blade analysis by Hodges [4] and by Bauchau and Guernsey [5]. In [5], the modal reduction accuracy of mixed elements was studied, but disappointing results were obtained, especially for torsional response, even when the mixed elements were supplemented by perturbation modes [6].

Although mixed elements displayed poor modal reduction accuracy in an earlier study, it may be shown that the method is algorithmically similar to the axial elongation variable, which reportedly has excellent modal reduction accuracy. It therefore seemed appropriate to give mixed elements a second look, which is the subject of this paper. In what follows, a rationale for the use of mixed elements is developed starting from the well-known Hodges-Dowell equations of a rotor blade specialized to axial and flap motions. The derivation of a mixed element is then described, and the element's effectiveness in modal reduction is illustrated with an articulated blade model. Finally, the study's conclusions are presented.

2. RATIONALE FOR MIXED ELEMENTS

2.1. Preliminaries: Hodges-Dowell Flap-Axial Blade Equations

The starting point for developing a rationale for mixed elements is the Hodges-Dowell blade equations [7] specialized to coupled axial-flap motions:

$$V_x' = -m\Omega^2 x - f_x, \tag{2.1}$$

$$m\ddot{w} = (V_x w')' - (EI_y w'')'' + f_z, \tag{2.2}$$

where V_x is the axial force, m is the mass per unit length, x is the axial coordinate, Ω is the rotor angular speed, w is the flap displacement, EI_y is the cross-section flap flexural rigidity, and f_x and f_z are applied forces per unit length. Following the usual conventions in the rotorcraft literature, a prime ($'$) denotes partial differentiation with respect to the axial coordinate, and a

dot $(\cdot)$ denotes partial differentiation with respect to time. If the blade is clamped at the spin axis, the boundary conditions are

$$w|_{x=0} = w'|_{x=o} = 0. \tag{2.3}$$

These equations are particularly useful for examining blade analysis methods because they are simple enough to permit easy inspection, yet they embody the coupling between axial and flap degrees of freedom, which is the key problem in applying modal reduction to rotor blade equations.

In what follows, several mathematical formulations for rotor blade analysis are presented, culminating with a mixed element. The formulations are evaluated based on their treatment of axial motions, and the key features of the mixed element are introduced in a step-by-step fashion.

2.2. Method 1: The Axial Displacement Variable

This method represents all variables in terms of displacement fields, and then applies polynomial discretizations of the fields over subregions of the model, which are simply finite elements. The following expression for axial force is used, which is consistent with the Hodges-Dowell ordering scheme

$$V_x = EA\left(u' + \frac{1}{2}w'^2\right), \tag{2.4}$$

where EA is the axial stiffness of the blade cross section. Substituting equation (2.4) into the Hodges-Dowell equations gives

$$m\ddot{u} = \left[EA\left(u' + \frac{1}{2}w'^2\right)\right]' + m\Omega^2 x + f_x, \tag{2.5}$$

$$m\ddot{w} = \left[EA\left(u' + \frac{1}{2}w'^2\right)w'\right]' - (EI_y w'')'' + f_z, \tag{2.6}$$

where $m\ddot{u}$ is formally negligible, but is included here for consistency with other treatments in the literature. The boundary conditions for a blade clamped at the spin axis are

$$u|_{x=0} = w|_{x=0} = w'|_{x=0} = 0. \tag{2.7}$$

Equations (2.5) and (2.6) allow for full discretization of the blade model in the axial direction, thereby permitting the full power of the finite-element method to be brought to bear on the analysis. Unfortunately, a high price for this flexibility stems from the difficulty of approximating the axial force, which is critical for accurately representing the blade bending stiffness. The source of the difficulty is that the constituent parts of the axial strain, $\epsilon_x = V_x/EA = u' + (1/2)w'^2$, are opposite and nearly equal whenever the flap displacement becomes significant; i.e., $u' \simeq -(1/2)w'^2$, and therefore, $|\epsilon_x| \ll |u'|$ and $|\epsilon_x| \ll w'^2$. In other words, ϵ_x is the small difference of much larger quantities, and computing it accurately requires far more accuracy in both u' and w'^2 than can be obtained by representing either of these using a small number of eigenmodes.

The problem encountered with the displacement approach will now be illustrated using several computational examples. The blade model used is shown in Figure 1. Consider first, an eigenanalysis of the spinning blade. For this analysis, *in vacuo* conditions are assumed, along with zero swashplate angles, and the blades' modes are computed about steady-state spin. Then, the static response of the blade, in modal space, is computed for tip flap loads of 2539.6 pounds and 5079.2 pounds, which correspond to coning angles of 4° and 8°, respectively. These are typical of the mean coning angles in rotorcraft under flight conditions (see [8]). The modal basis contains the first two flap modes, while the number of axial modes were varied to study the convergence of the first two flap frequencies. The flap frequencies are plotted against the number of axial modes in Figure 2. Note that 30 axial modes completely fill the axial displacement subspace of

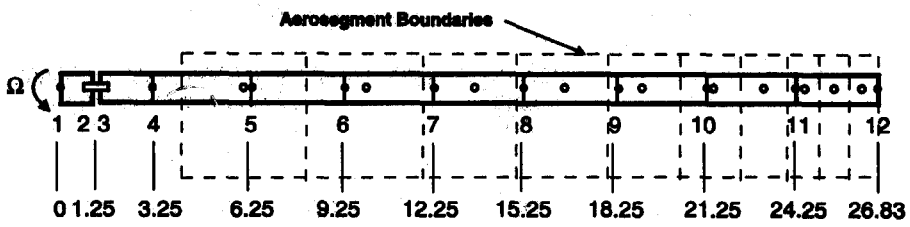

Structural Properties	Aerodynamic Properties	Flight Conditions
Radius - 26.83 ft. EI_y - 1.85E5 lb-ft^2 EI_z - 4.18E5 lb-ft^2 GJ - 2.08E5 lb-ft^2 EA - 6.69E8 lb 92 DOF's	SC1095 Airfoil Uniform Inflow Greenberg Aerodynamics Chord - 1.7405 ft	Ω=258 rev/minute θ_0=10.0 deg. θ_C=2.0 deg. θ_S=-7.0 deg. Θ=4.0 deg. Ψ=Φ=0.0 deg. μ=.373, C_T/σ=.072

Figure 1. Articulated blade model.

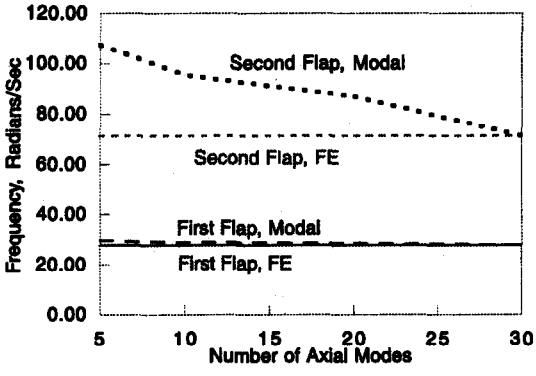

(a) Four degrees coning angle.

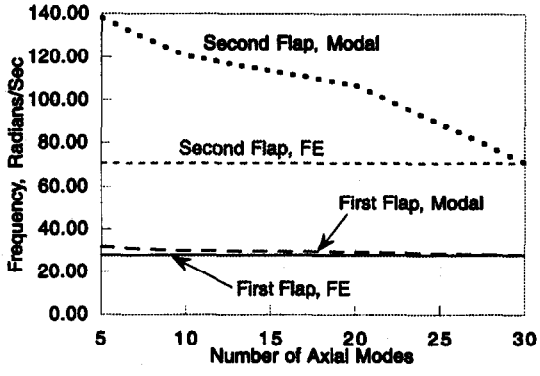

(b) Eight degrees coning angle.

Figure 2. Articulated blade flap frequencies: displacement elements.

Table 1. Articulated blade modes.

Mode ID	Frequency (/rev)
First lag	0.27
First flap	1.03
Second flap	2.63
Second lag	4.09
First torsion	4.86
Second torsion	14.59
First axial	22.12
Second axial	66.41

the model. It may be seen that while reasonable results are obtained for the first flap frequency with just a few axial modes, the accuracy of the second flap frequency is much poorer, and does not become acceptable until almost the entire axial subspace is filled.

To further illustrate the problems of the axial displacement variable, consider the periodic solution of the model shown in Figure 1. The *in vacuo* eigenmodes of this model are given in Table 1, and the modal bases used in the calculations are given in Table 2. Note that

Table 2. Description of modal bases.

Modal Basis	Number of Modes			
	Lag	Flap	Torsion	Axial
1l, 1f, 1t, 1a	1	1	1	1
2l, 2f, 2t, 2a	2	2	2	2

in contrast to the theory presented earlier, the model is constrained so that all motions—not just flap and axial—are permitted. Periodic solutions for the degrees of freedom at the tip node are shown in Figure 3. It may be seen that the agreement between between the modal and finite-element solutions is quite poor for the flap, lag, and axial displacements, as was expected. But surprisingly, the agreement between the finite-element and modal solutions is quite good for the pitch rotation. The reasons for the good modal approximations are the high torsional stiffness of the blade, combined with the low degree of bending-torsion coupling in stiff, articulated blades of the type analyzed here. Since the pitch response of the blade is the main contributor to the aerodynamic angle of attack, the good modal approximation for pitch implies that the poor results for the bending and axial motions must come from errors made in computing those motions, rather than from erroneous aerodynamic loading. Therefore, the approach taken here in focusing on bending-axial response to evaluate blade formulations is fully justified.

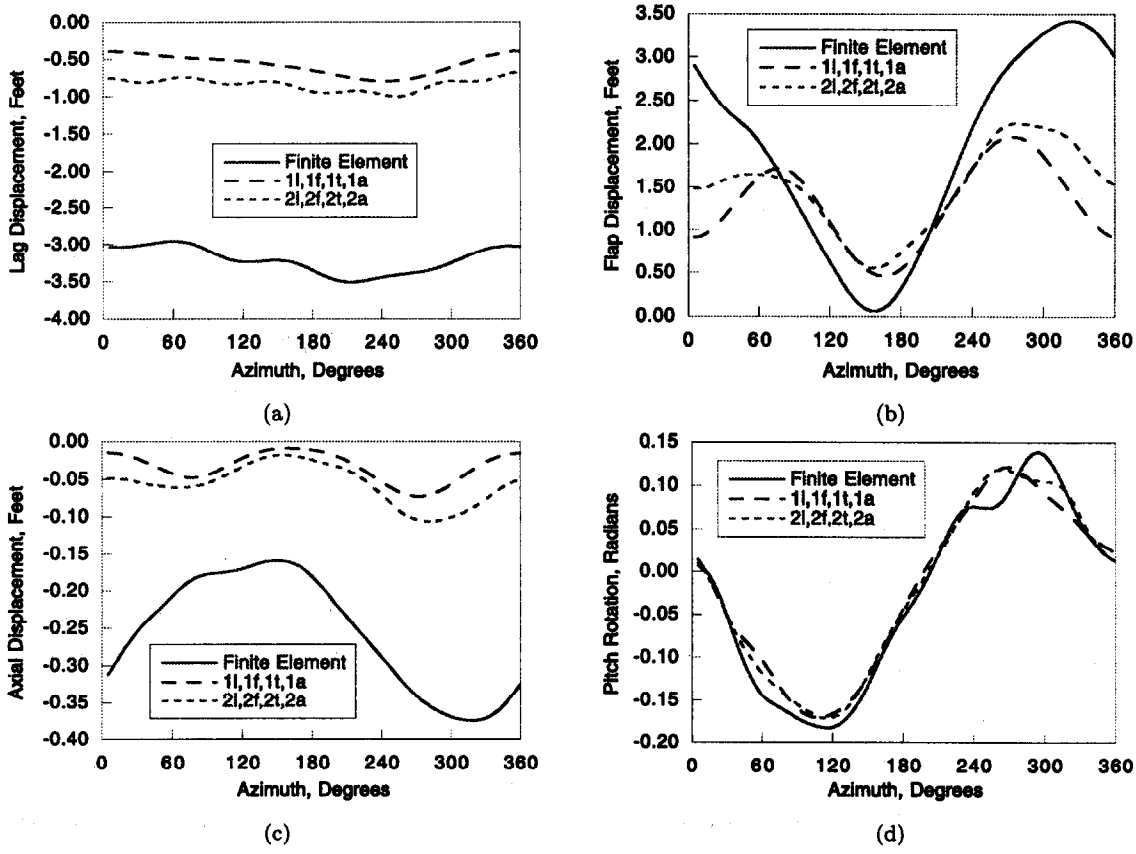

Figure 3. Articulated blade tip deflections: displacement elements.

2.3. Method 2: The Axial Force Variable

One approach to modifying the analysis formulation to facilitate modal reduction involves parameterizing the axial motion using the axial force rather than the axial displacement. The

axial displacement may be written in terms of the axial force using equation (2.4):

$$u' = \frac{V_x}{EA} - \frac{1}{2}w'^2 \tag{2.8}$$

or

$$u = \int_0^x \left(\frac{V_x}{EA} - \frac{1}{2}w'^2\right) ds. \tag{2.9}$$

With this reparameterization, the axial force is now expressed as a single variable, and the numerical conditioning problems associated with the axial displacement variable are absent.

The need for an additional improvement to the analysis procedure becomes evident upon applying the axial force variable to the Hodges-Dowell equations. Substituting equation (2.9) into equations (2.5) and (2.6) gives

$$m\int_0^x \left(\frac{\ddot{V}_x}{EA} - \dot{w}'^2 - w'\ddot{w}'\right) ds = V_x' + m\Omega^2 x + f_x, \tag{2.10}$$

$$m\ddot{w} = (V_x w')' - (EI_y w'')'' + f_z. \tag{2.11}$$

Simplifying equations (2.10) and (2.11) by removing the negligible terms arising from $m\ddot{u}$ leads, once again, to the Hodges-Dowell equations (equations (2.1) and (2.2)). An examination of those equations reveals a quadratic nonlinearity, $(V_x w')'$, which is significant enough to adversely impact modal reduction. Indeed, it was found that a mixed element formulated analogously to equation (2.11) had only modestly improved modal reduction capabilities in comparison with the displacement element. This problem may be removed by expressing the variables as sums of steady-state values and dynamic perturbations:

$$V_x = V_{x_0} + \Delta V_x, \tag{2.12}$$

$$w = \Delta w. \tag{2.13}$$

For simplicity, let the external forces be associated with the perturbations, viz.,

$$f_x = \Delta f_x, \tag{2.14}$$

$$f_z = \Delta f_z. \tag{2.15}$$

Substituting these representations into equations (2.10) and (2.11) and placing linear terms on the left-hand side gives

$$\Delta V_x' = \Delta f_x, \tag{2.16}$$

$$m\Delta\ddot{w} - (V_{x_0}\Delta w')' - (\Delta V_x w_0')' + (EI_y \Delta w'')'' = (\Delta V_x \Delta w')' + \Delta f_z. \tag{2.17}$$

Inasmuch as the axial force in a rotor blade varies little from its steady-state value, the only nonlinear term appearing in these equations, $(\Delta V_x \Delta w')'$, will be quite small.

Although the axial force variable has not been applied to rotor blades in the form described here, its likely effectiveness in modal reduction may be inferred from the success of a similar concept, the *axial elongation variable*, which is defined as

$$u_e = \int_0^x \frac{V_x}{EA}\, ds. \tag{2.18}$$

Clearly, the underlying motivations of the axial force and axial elongation variables, insofar as they treat axial forces, are identical and their implementations are quite similar. The effectiveness of the axial elongation variable at modal reduction has been well documented [1]. Although the

axial elongation variable is the preferred parameterization in rotorcraft practice, the axial force variable is preferred in this paper because it is consistent with the literature on mixed elements.

Although the axial force variable should greatly facilitate modal reduction of the blade equations, this improvement comes at the expense of introducing a modeling problem: the axial deflection must be computed by integrating the axial force outward from the spin axis, as implied by equation (2.9). This means that the information needed to compute an element's kinematics will not be available until all elements closer to the spin axis have been processed. Conversely, the element's forces cannot be assembled into the model until all outboard elements have been processed. For example, equation (2.9) implies that the axial displacement of the root of the n^{th} element outboard from the spin axis in a single load path blade must be computed as follows:

$$u = \sum_{i=1}^{n-1} \int_0^x \left(\frac{V_x}{EA} - \frac{1}{2} w'^2 \right)_i ds, \tag{2.19}$$

where the subscript i signifies the i^{th} element outboard from the spin axis. In order to satisfy this equation, the standard finite-element assembly process based on linear transformations of system degrees of freedom at nodes contiguous to the element must be replaced by a more complex process.

A more serious consequence of computing the axial response using equation (2.19) is that that quantity is uniquely defined only when a single load path is present; in other words, it is applicable only to blade models with a *tree topology*. Special procedures are required to handle multiple load paths, which occur in bearingless rotors, but which also can arise in blades of any configuration when they are modeled using two- or three-dimensional elements. This problem should come as no surprise, because it is well known (see [9]) that analysis methodologies that employ forces as unknowns require special—often awkward—adjustments when treating redundant models. A discussion of a related subject, the analytical problems caused by a quasi-coordinate such as the axial elongation u_e, has been given by Hodges *et al.* [10]. Although the axial displacement variable is not well suited to modal reduction, it requires no special adjustments for redundant models, and in general, it is much easier to apply to complex topologies than solution methodologies that employ forces—or in the case of the axial elongation variable, force-like quantities—as variables.

2.4. Method 3: Axial Force *and* Axial Displacement Variables—A Mixed Element

It has been shown that parameterizing axial motions using the Lagrangian axial displacement gives unrestricted modeling freedom at the expense of ill-conditioned and highly nonlinear axial-bending coupling, while using the axial force as a variable makes modeling more awkward, but simplifies axial-bending coupling. We will now seek to obtain the advantages of both methods—without their limitations—by using both axial displacements *and* axial forces as variables. That may be accomplished by augmenting the Hodges-Dowell equations with an equation that relates the axial force and the axial displacement. Three equations result:

$$\frac{V_x}{EA} = u' + \frac{1}{2} w'^2, \tag{2.20}$$

$$m\ddot{u} = V_x' + m\Omega^2(x + u) + f_x, \tag{2.21}$$

$$m\ddot{w} = (V_x w')' + f_z. \tag{2.22}$$

Since axial forces *and* displacements are variables in these equations, it is dubbed a *mixed element*.

The advantages of the mixed-element equations are more readily appreciated when they are expressed in variational form. That process involves applying finite-element interpolations to the three independent variables: $V_x = [H_{V_x}]\{q_{V_x}\}$, $u = [H_u]\{q_u\}$, and $w = [H_w]\{q_w\}$. In what follows, all variables are assumed to have been discretized, but—when possible—they are displayed as continuous for improved readability. The finite-element interpolations are substituted

into equations (2.20)–(2.22), which are then are multiplied by δV_x, δu, and δw, respectively. The results of these operations are then summed and integrated over the length of the element giving

$$\int_0^l \left(\{\delta q_{V_x}\}^\top \{\bar{Y}_{V_x}\} + \{\delta q_u\}^\top \{\bar{Y}_u\} + \{\delta q_w\}^\top \{\bar{Y}_w\} \right) dx = 0, \tag{2.23}$$

where

$$\{\bar{Y}_{V_x}\} = [H_{V_x}]^\top \left(\frac{V_x}{EA} - u' - \frac{1}{2} w'^2 \right), \tag{2.24}$$

$$\{\bar{Y}_u\} = [H_u]^\top [m\ddot{u} - V_x' - m\Omega^2(x+u) - f_x], \tag{2.25}$$

$$\{\bar{Y}_w\} = [H_w]^\top \left[m\ddot{w} - (V_x w')' - f_z \right]. \tag{2.26}$$

For future reference, note that it is often convenient to express the discretized form of u' as follows:

$$u' = [H_u'] \{q_u\} = [H_{u'}] \{q_{u'}\}, \tag{2.27}$$

for some set of unknowns $\{q_{u'}\}$, which is of size $N_u - 1$.

The usefulness of the mixed element for modal reduction may be inferred from arguments similar to those used in discussing the axial force variable. First, consider the $\{\delta q_u\}$ variation. Setting the coefficient of that variation to zero gives, after removing the small contributions from u, and $\ddot{u}$,

$$\int_0^l [H_u]^\top \left[V_x' - m\Omega^2(x+u) - f_x \right] dx = 0, \tag{2.28}$$

which is analogous to the first of the Hodges-Dowell equations, and which largely determines V_x. Thus, in contrast to the axial displacement variable method, the axial force, which is a key quantity, is determined directly from what is essentially an equilibrium equation. Using V_x in the $\{\delta q_w\}$ variation gives

$$\int_0^l [H_w]^\top \left[m\ddot{w} - (V_x w')' - f_z \right] dx = 0, \tag{2.29}$$

which is analogous to the second of the Hodges-Dowell equations, and which largely determines w. Finally, the $\{\delta q_{V_x}\}$ variation leads to

$$\int_0^l [H_{V_x}]^\top \left(\frac{V_x}{EA} - u' - \frac{1}{2} w'^2 \right) dx = 0, \tag{2.30}$$

which is analogous to equation (2.9), and which largely determines u. Observe that *weak enforcement* of the governing equations is crucial in allowing the axial force to be computed as a separate variable. Also, weak enforcement of the force-displacement equation (equation (2.30)) permits the implicit determination of u from that equation and eliminates the need to constrain the model's topology in order to be able to calculate u by integrating outward from the spin axis as in equation (2.9).

The axial force variable was a key motivation for the mixed element, but a stronger relationship between the two methods can be proven: if the axial force variable method is applicable, it can be made *mathematically equivalent* to the mixed element. Substituting for u in equation (2.30) and rearranging terms gives

$$\left(\int_0^l [H_{V_x}]^\top [H_{u'}] \, dx \right) \{q_{u'}\} = \int_0^l [H_{V_x}]^\top \left(\frac{V_x}{EA} - \frac{1}{2} w'^2 \right) dx. \tag{2.31}$$

Convergence considerations dictate that (see [11])

$$N_u - 1 = N_{V_x}, \tag{2.32}$$

and recalling that $\{q_{u'}\}$ is of length $N_u - 1$, it may be concluded that the coefficient of $\{q_{u'}\}$ in equation (2.31) is a square matrix. Since that matrix should also be nonsingular in a properly formulated element, equation (2.31) can be solved for $\{q_{u'}\}$ as follows:

$$\{q_{u'}\} = \left(\int_0^l [H_{V_x}]^\top [H_{u'}]\, dx\right)^{-1} \int_0^l [H_{V_x}]^\top \left(\frac{V_x}{EA} - \frac{1}{2}w'^2\right) dx. \tag{2.33}$$

Now look back at equation (2.8), which was used for the axial force variable method. It is evident that if that equation is weakly enforced, and if u, V_x, and w are interpolated as in the mixed element, then it will yield an expression for $\{q_{u'}\}$, hence u, that is identical to equation (2.8). Finally, substituting for u in the axial force variable and mixed-element methods will show that both yield identical expressions for V_x and w.

3. DEVELOPMENT OF A MIXED ELEMENT FOR ROTOR BLADES

The mixed element developed thus far suffers two shortcomings: it is valid only for flap-axial motions, and it has been justified in a rather *ad hoc* fashion. In this section, a general purpose mixed element for rotor blades with coupled flap-lag-axial-torsional motions is derived from a variational principle. The element has been implemented in an experimental version of the Second Comprehensive Generation Helicopter Analysis System (2GCHAS) [12].

In essence, the finite element already used in 2GCHAS for rotor blade analysis, the so-called "nonlinear beam element", was converted into a mixed element. In contrast to other mixed elements that have been used for rotor blades (see [4,5]), the mixed treatment is limited to the axial direction. This limitation reduces the number of degrees of freedom that are needed and simplifies both the derivation and the programming of the element. Only the structural terms of the 2GCHAS element are impacted by the conversion to a mixed element, and therefore, only those terms are derived here. But for the sake of completeness, the element's inertia terms are derived in the Appendix.

The conversion process proved to be quite fast and straightforward, as the reader may infer by comparing the theory of the mixed element with the theory of the original 2GCHAS element and noting the strong parallelism between the two. The ease of conversion is stressed here because it should be duplicated for *any* displacement-based finite-element code, and not just 2GCHAS, and underscores the utility of mixed elements. The derivation presented here employs the notations and conventions of the 2GCHAS, and the reader should consult [12] for the necessary background material.

3.2. Element Geometry and Kinematics

3.2.1. Element geometry

The geometry of the undeformed element is shown in Figure 4. The element is assumed to move in a noninertial reference frame denoted E, whose motion relative to the inertial frame I is prescribed. The E frame absorbs the large rigid-body motions of the rotorcraft, while the smaller motions of the deforming blade relative to the frame are analyzed using a "moderate deformation" blade theory familiar to rotorcraft analysts. The geometry and motion of the element are defined with the aid of a coordinate system within the E frame with basis vectors $\{\mathbf{b}_1^E, \mathbf{b}_2^E, \mathbf{b}_3^E\}$. The beam element reference axis is assumed to be initially straight and parallel

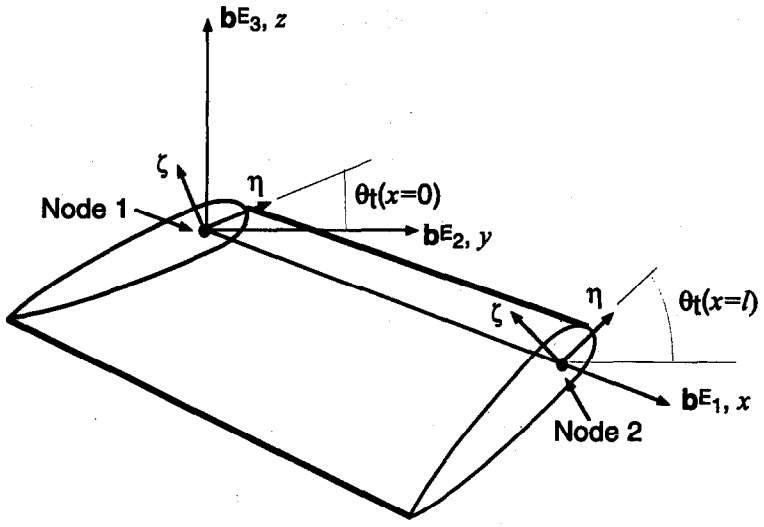

Figure 4. Geometry of undeformed element.

to the unit vector $\mathbf{b}_1^E$. A structural reference frame S is located on the reference axis a distance x from the origin of the E frame. Its orientation differs from E by a rotation about $\mathbf{b}_1^E$ by the built-in twist angle θ_t, rotating the E frame coordinates y and z into alignment with S frame cross-sectional coordinates η and ζ (see Figure 4). Thus, the position and orientation of S with respect to E are

$$\{r_E^{SE}\} = \lfloor x, 0, 0 \rfloor^\top,$$
$$[T^{SE}] = \begin{bmatrix} 1 & 0 & 0 \\ 0 & \cos\theta_t & \sin\theta_t \\ 0 & -\sin\theta_t & \cos\theta_t \end{bmatrix}. \tag{3.34}$$

3.2.2. Element kinematics

In this section, the displacement of a generic material point A within the undeformed beam is developed; in the deformed beam, it is denoted by A'. In order to carry out this development, consider first the motion of E in I. Then, the 3-D displacement field of the beam is represented in terms of 1-D variables and cross-sectional position coordinates. An intermediate frame S' is introduced and used to relate the motion of A' to I.

The deformed beam cross-sectional frame S', which becomes coincident with S when the beam is in its undeformed state, is specified in the following way. The material points in the undeformed beam which lie along the reference line move when the beam deforms, deforming into a curved line which is not, in general, the same length as the original reference line because of the possibility of stretching. Similarly, the material points in the plane perpendicular to the reference line are denoted as the reference cross-section. This plane of points, determined by the η and ζ coordinate directions, also moves when the beam deforms. The points remain contiguous in the deformed beam so that they make up a surface which is very close to a plane.

In accordance with Euler-Bernoulli beam theory, it is assumed that the frame S' rigidly transports the η and ζ coordinate directions at any particular value of x to a new orientation, perpendicular to the reference line of the deformed beam at the same material point (which is associated with the same value of x in the undeformed beam). Any deviation of the surface of points from a plane is, in accordance with Euler-Bernoulli theory, small. The orientation of S' in E can be expressed in terms of a set of 1-D variables which govern the position of and the rotation of S' about the deformed beam reference line.

As expected, three rotations are sufficient to express the direction cosines of S' in E, denoted by $[T^{S'E}]$. A set of body 3: 3-2-1 orientation angles [13] is used. The direction cosine matrix

$[T^{S'E}]$ may be expressed in terms of these angles as

$$\left[T^{S'E}\right] = \begin{bmatrix} 1 & 0 & 0 \\ 0 & c_1 & s_1 \\ 0 & -s_1 & c_1 \end{bmatrix} \begin{bmatrix} c_2 & 0 & -s_2 \\ 0 & 1 & 0 \\ s_2 & 0 & c_2 \end{bmatrix} \begin{bmatrix} c_3 & s_3 & 0 \\ -s_3 & c_3 & 0 \\ 0 & 0 & 1 \end{bmatrix},$$

where $s_1 = \sin\theta_1$, $c_1 = \cos\theta_1$, etc., resulting in

$$\left[T^{S'E}\right] = \begin{bmatrix} c_3c_2 & c_2s_3 & -s_2 \\ -s_3c_1 + s_1s_2c_3 & c_1c_3 + s_1s_2s_3 & s_1c_2 \\ s_1s_3 + c_1c_3s_2 & -c_3s_1 + c_1s_3s_2 & c_1c_2 \end{bmatrix}. \tag{3.35}$$

The orientation of S' with respect to E is now expressible as

$$\begin{Bmatrix} \mathbf{b}_1^{S'} \\ \mathbf{b}_2^{S'} \\ \mathbf{b}_3^{S'} \end{Bmatrix} = \left[T^{S'E}\right] \begin{Bmatrix} \mathbf{b}_1^{E} \\ \mathbf{b}_2^{E} \\ \mathbf{b}_3^{E} \end{Bmatrix}. \tag{3.36}$$

Upon expressing the direction cosines in equation (3.35) in terms of the 1-D variables v', w', and ϕ, and retaining terms to $O(\epsilon^2)$, the transformation matrix $[T^{S'E}]$ becomes (see [10])

$$\left[T^{S'E}\right] = \begin{bmatrix} 1 - \dfrac{v'^2}{2} - \dfrac{w'^2}{2} & v' & w' \\ -(v'c_1 + w's_1) & c_1\left(1 - \dfrac{v'^2}{2}\right) - v'w's_1 & s_1\left(1 - \dfrac{w'^2}{2}\right) \\ v's_1 - w'c_1 & -s_1\left(1 - \dfrac{v'^2}{2}\right) - v'w'c_1 & c_1\left(1 - \dfrac{w'^2}{2}\right) \end{bmatrix}. \tag{3.37}$$

The position of the generic point A' on the deformed beam cross-section is then defined as

$$\begin{aligned} \mathbf{r}^{A'I} &= \mathbf{r}^{EI} + \mathbf{r}^{A'E} \\ &= \mathbf{r}^{EI} + (x+u)\mathbf{b}_1^E + v\mathbf{b}_2^E + w\mathbf{b}_3^E + \Psi\kappa_x\mathbf{b}_1^{S'} + \eta\mathbf{b}_2^{S'} + \zeta\mathbf{b}_3^{S'}. \end{aligned} \tag{3.38}$$

This equation can be written in column matrix form if each vector is expressed in terms of its measure numbers in the E basis, viz.,

$$\begin{aligned} \left\{r_E^{A'I}\right\} &= \left\{r_E^{EI}\right\} + \left\{r_E^{A'E}\right\} \\ &= \left\{r_E^{EI}\right\} + \begin{Bmatrix} x+u \\ v \\ w \end{Bmatrix} + \left[T^{ES'}\right] \begin{Bmatrix} \Psi\kappa_x \\ \eta \\ \zeta \end{Bmatrix}. \end{aligned} \tag{3.39}$$

Here u, v, and w are the displacement measures of the beam reference line due to elastic deformations in the E frame, $x\mathbf{b}_1^E$ is the vector from the origin of the element frame E to the origin of the structural frame S (see Figure 5), and η and ζ are the cross-sectional position coordinates. The last term is the position of A' within the deformed beam cross-sectional frame S'. (Recall that these coordinates have been convected, and thus, they correspond to the original cross-sectional coordinates of A in the undeformed beam.) Finally, an out-of-plane warping is assumed to be of the form $\kappa_x(x)\Psi(\eta,\zeta)$, where Ψ is the St. Venant torsional warping function and $\kappa_x(x)$ represents the amplitude of the warping [14]. Subsequently, κ_x is defined as the elastic part of twist per unit length or just "elastic twist".

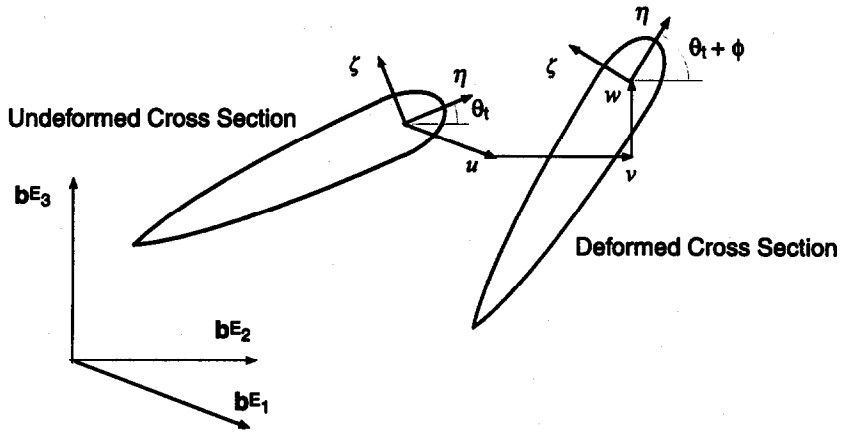

Figure 5. Undeformed and deformed element cross-section.

3.3. Stress-Strain Relationship

The stress-strain relationship for a linearly elastic anisotropic solid is characterized by 21 constants which form a fourth-order tensor. The 21 material constants can be obtained in the local Cartesian system along unit vectors $\mathbf{b}_i^S$, associated with the curvilinear coordinates x, η, and ζ. These material constants can be formed into a 6×6 symmetric matrix, the elements of which may vary as functions of x, η, and ζ. This matrix linearly relates the stress components σ_{xx}, $\sigma_{\eta\eta}$, $\sigma_{\zeta\zeta}$, $\sigma_{\eta\zeta}$, $\sigma_{x\zeta}$, and $\sigma_{x\eta}$, with the strain components γ_{xx}, $\gamma_{\eta\eta}$, $\gamma_{\zeta\zeta}$, $\gamma_{\eta\zeta}$, $\gamma_{x\zeta}$, and $\gamma_{x\eta}$, where the order of the components corresponds to that of anisotropic elasticity.

For slender, isotropic beams, the Bernoulli hypothesis approximately holds, according to asymptotic analyses [15]. This hypothesis is that the transverse normal stresses $\sigma_{\eta\eta}$ and $\sigma_{\zeta\zeta}$, along with the distortion shear stress $\sigma_{\eta\zeta}$, are much smaller than the other three stress components. Thus, one solves for the three strain components $\gamma_{\eta\eta}$, $\gamma_{\eta\zeta}$, and $\gamma_{\zeta\zeta}$ in terms of the others. Substituting the results into the original equations for σ_{xx}, $\sigma_{x\eta}$, and $\sigma_{x\zeta}$, one obtains a "reduced" 3-D stress-strain law which can be written as

$$\begin{Bmatrix} \sigma_{xx} \\ \sigma_{x\eta} \\ \sigma_{x\zeta} \end{Bmatrix} = \begin{bmatrix} Q_{11} & Q_{16} & Q_{15} \\ Q_{16} & Q_{66} & Q_{56} \\ Q_{15} & Q_{56} & Q_{55} \end{bmatrix} \begin{Bmatrix} \gamma_{xx} \\ \gamma_{x\eta} \\ \gamma_{x\zeta} \end{Bmatrix} = [Q]\{\Gamma\}. \tag{3.40}$$

This reduced 3-D stress-strain law is the basis of most elementary beam theories. Some published treatments confuse this with setting the *strain* components $\gamma_{\eta\eta}$, $\gamma_{\eta\zeta}$, and $\gamma_{\zeta\zeta}$ equal to zero. These are not zero, but may be calculated from the above reduction process.

Note that, in the special case of the beam having laminated construction with the ζ direction perpendicular to the plane of the laminate, this numbering scheme corresponds to that of common treatments of lamination theory. Note that, for the case of an isotropic material,

$$\begin{aligned} Q_{11} &= E, \\ Q_{55} &= Q_{66} = G, \\ Q_{15} &= Q_{16} = Q_{56} = 0. \end{aligned} \tag{3.41}$$

With the above 3-D stress-strain law, one can write the strain energy per unit length (or 1-D strain energy function),

$$\Phi = \frac{1}{2}\left\langle \{\Gamma\}^{\mathsf{T}}[Q]\{\Gamma\} \right\rangle, \tag{3.42}$$

where $\langle(\bullet)\rangle$ refers to an integral of $(\bullet)$ over the cross-section, which forms the basis for beam theory. In order to determine the 1-D function Φ, the strain field must be expressed in such a

way that this cross-sectional integral can be evaluated. Note that the strain energy of the element is simply

$$U = \int_0^\ell \Phi \, dx. \tag{3.43}$$

3.4. 1-D Strain Energy Function

From axiomatic, Euler-Bernoulli rod theory, the strain energy density of the beam element (i.e., strain energy per unit length) may be written in the following form:

$$\Phi = \frac{1}{2} \begin{Bmatrix} \epsilon_x \\ \kappa_x \\ \kappa_\eta \\ \kappa_\zeta \end{Bmatrix}^{\mathsf{T}} \begin{bmatrix} E_0 A & E_0 D_0 & E_0 A e_{t_\zeta} & -E_0 A e_{t_\eta} \\ E_0 D_0 & G_0 J & E_0 D_3 & -E_0 D_2 \\ E_0 A e_{t_\zeta} & E_0 D_3 & E_0 I_\eta & E_0 I_{\eta\zeta} \\ -E_0 A e_{t_\eta} & -E_0 D_2 & E_0 I_{\eta\zeta} & E_0 I_\zeta \end{bmatrix} \begin{Bmatrix} \epsilon_x \\ \kappa_x \\ \kappa_\eta \\ \kappa_\zeta \end{Bmatrix}, \tag{3.44}$$

where ϵ_x, κ_x, κ_η, and κ_ζ are generalized beam strains and curvatures defined by

$$\begin{aligned} \epsilon_x &= s' - 1, \\ \kappa_x &= \left(\mathbf{b}_2^{S'}\right)' \cdot \mathbf{b}_3^{S'} - \theta_t', \\ \kappa_\eta &= -\left(\mathbf{b}_1^{S'}\right)' \cdot \mathbf{b}_3^{S'}, \\ \kappa_\zeta &= \left(\mathbf{b}_1^{S'}\right)' \cdot \mathbf{b}_2^{S'}. \end{aligned} \tag{3.45}$$

Equation (3.44) is adequate for the stiff, articulated blade considered in this paper, but note that for bearingless blades, it must be augmented by an additional nonlinear strain term that gives rise to the so-called "trapeze effect (see [16]).

For elements composed of isotropic materials, the cross-sectional constants in equation (3.45) may be computed as follows. Substitute the displacement obtained from the element's kinematical relations (equations (3.37) and (3.39)) into small strain, moderate rotation strain-displacement relations that can adequately capture rotor blade kinematics (see [17]). Next, substitute the strains into equation (3.10) to compute the stresses, and then integrate the stresses over the cross-section to obtain forces and moments. This process gives

$$A = \frac{1}{E_0} \langle Q_{11} \rangle, \qquad k_A^2 = \frac{1}{A} \left(I_\eta + I_\zeta \right),$$

$$e_{t_\eta} = \frac{1}{E_0 A} \langle Q_{11} \eta \rangle, \qquad e_{t_\zeta} = \frac{1}{E_0 A} \langle Q_{11} \zeta \rangle,$$

$$I_\zeta = \frac{1}{E_0} \langle Q_{11} \eta^2 \rangle, \qquad I_\eta = \frac{1}{E_0} \langle Q_{11} \zeta^2 \rangle,$$

$$I_{\eta\zeta} = -\frac{1}{E_0} \langle Q_{11} \eta\zeta \rangle, \qquad B_1 = \frac{1}{E_0} \left\langle Q_{11} \left(\eta^2 + \zeta^2 \right)^2 \right\rangle,$$

$$B_2 = \frac{1}{E_0} \left\langle Q_{11} \eta \left(\eta^2 + \zeta^2 \right) \right\rangle, \qquad B_3 = \frac{1}{E_0} \left\langle Q_{11} \zeta \left(\eta^2 + \zeta^2 \right) \right\rangle,$$

$$D_0 = \frac{1}{E_0} \langle Q_{1s} \rangle \frac{1}{E_0} \theta_t' \left\langle Q_{11} \left(\zeta \Psi_{,\eta} - \eta \Psi_{,\zeta} \right) \right\rangle, \qquad D_1 = \frac{1}{E_0} \left\langle \left(\eta^2 + \zeta^2 \right) Q_{1s} \right\rangle + \frac{1}{E_0} \theta_t' \left\langle \left(\eta^2 + \zeta^2 \right) Q_{11} \left(\zeta \Psi_{,\eta} - \eta \Psi_{,\zeta} \right) \right\rangle,$$

$$D_2 = \frac{1}{E_0} \langle Q_{1s} \eta \rangle + \frac{1}{E_0} \theta_t' \left\langle \eta Q_{11} \left(\zeta \Psi_{,\eta} - \eta \Psi_{,\zeta} \right) \right\rangle, \qquad D_3 = \frac{1}{E_0} \langle Q_{1s} \zeta \rangle + \frac{1}{E_0} \theta_t' \left\langle \zeta Q_{11} \left(\zeta \Psi_{,\eta} - \eta \Psi_{,\zeta} \right) \right\rangle,$$

$$J = \frac{1}{G_0} \left\langle Q_{55} \left(\Psi_{,\zeta} + \eta \right)^2 + 2 Q_{56} \left(\Psi_{,\eta} - \zeta \right) \left(\Psi_{,\zeta} + \eta \right) + Q_{66} \left(\Psi_{,\eta} - \zeta \right)^2 \right\rangle$$

$$+ \frac{1}{G_0} \theta_t'^2 \left\langle Q_{11} \left(\zeta \Psi_{,\eta} - \eta \Psi_{,\zeta} \right)^2 \right\rangle + 2 \frac{1}{G_0} \theta_t' \left\langle \left(\zeta \Psi_{,\eta} - \eta \Psi_{,\zeta} \right) \left[Q_{15} \left(\Psi_{,\zeta} + \eta \right) + Q_{16} \left(\Psi_{,\eta} - \zeta \right) \right] \right\rangle,$$

where $Q_{1s} = Q_{15}(\Psi_{,\zeta} + \eta) + Q_{16}(\Psi_{,\eta} - \zeta)$. For an element composed of anisotropic materials, three-dimensional effects such as inplane warping become significant, and elementary beam theory is inadequate for computing the cross-sectional constants. However, even in this more complex case, a formal, asymptotic analysis shows that the *form* of equation (3.44) remains correct, and then the 4×4 matrix in equation (3.44) can be calculated using a code such as VABS [18], which may be applied to arbitrary cross-sectional geometry and material properties. In general, these properties depend on the cross-sectional geometry, the material anisotropy, and the local initial twist.

It is well known that the displacement-based element behaves poorly in modal reduction, and that this problem may be remedied by formulating the axial strain in terms of the axial force rather than the axial displacement. This may be accomplished by differentiating the strain energy with respect to the axial strain to obtain an expression for the axial force, and then using that expression to solve for the axial strain in terms of the axial force and the other generalized strains, viz.,

$$\epsilon_x = \frac{1}{A}\left(\frac{V_x}{E_0} - D_0\kappa_x - Ae_{t_\zeta}\kappa_\eta + Ae_{t_\eta}\kappa_\zeta\right). \tag{3.46}$$

Substituting equation (3.46) into equation (3.44) gives an expression for the strain energy in terms of the axial force V_x. It is important, however, that the axial strain somehow be reintroduced explicitly into the strain energy to exhibit its coupling with the finite-element axial degrees of freedom, but this must be done in a way that allows all the variables to be treated as independent, despite the redundancy between ϵ_x and V_x. This goal may be accomplished by appending equation (3.46) to the strain energy via a Lagrange multiplier, whereupon the strain energy becomes

$$\Phi = \frac{1}{2}\{\gamma^*\}^\top [K_0]\{\gamma^*\} + \lambda\left[\epsilon_x - \frac{1}{A}\left(\frac{V_x}{E_0} - D_0\kappa_x - Ae_{t\zeta}\kappa_\eta + Ae_{t\eta}\kappa_\zeta\right)\right], \tag{3.47}$$

where λ is a Lagrange multiplier, $\{\gamma^*\}$ is the reparameterized column matrix of generalized strains:

$$\{\gamma^*\} = \begin{Bmatrix} \frac{1}{A}\left(\frac{V_x}{E_0} - D_0\kappa_x - Ae_{t\zeta}\kappa_\eta + Ae_{t\eta}\kappa_\zeta\right) \\ \kappa_x \\ \kappa_\eta \\ \kappa_\zeta \end{Bmatrix}, \tag{3.48}$$

and $[K_0]$ is the coefficient matrix in equation (3.44):

$$[K_0] = \begin{bmatrix} E_0A & E_0D_0 & E_0Ae_{t_\zeta} & -E_0Ae_{t_\eta} \\ E_0D_0 & G_0J & E_0D_3 & -E_0D_2 \\ E_0Ae_{t_\zeta} & E_0D_3 & E_0I_\eta & E_0I_{\eta\zeta} \\ -E_0Ae_{t_\eta} & -E_0D_2 & E_0I_{\eta\zeta} & E_0I_\zeta \end{bmatrix}. \tag{3.49}$$

By taking the variation of Φ with respect to V_x, λ may be identified as the axial force, and therefore, the strain energy may be written as

$$\Phi = \frac{1}{2}\{\gamma^*\}^\top [K_0]\{\gamma^*\} + V_x\left[\epsilon_x - \frac{1}{A}\left(\frac{V_x}{E_0} - D_0\kappa_x - Ae_{t\zeta}\kappa_\eta + Ae_{t\eta}\kappa_\zeta\right)\right], \tag{3.50}$$

where ϵ_x is expressed in terms of the primal displacement variables u, v, w, and ϕ.

If the strain energy is used as shown in equation (5), it will be found that the coefficients of the equations pertaining to V_x will differ greatly from the other coefficients for typical rotor blades, and this raises the specter of ill-conditioning of the system equations. The coefficients of the element's equations may be made more uniform in magnitude by replacing V_x with a strain-like quantity defined as follows:

$$\bar{\epsilon} \equiv \frac{V_x}{E_0A}, \tag{3.51}$$

whereupon the strain energy becomes

$$\Phi = \frac{1}{2}\{\gamma^*\}^\top [K_0]\{\gamma^*\} + \bar{\epsilon}\left[E_0A(\epsilon_x - \bar{\epsilon}) + E_0D_0\kappa_x + E_0Ae_{t\zeta}\kappa_\eta - E_0Ae_{t\eta}\kappa_\zeta\right]. \tag{3.52}$$

3.5. Contributions from Strain Energy Function

In this section, the contributions to the equations of motion from strain energy are formulated. For this, the strain energy must be expressed in terms of the displacement and force variables of the analysis. The generalized internal loads are then obtained from the first variation of the strain energy function, and the contribution to the Jacobian is obtained from the second variation. Like the previous rendition of this element, which employed only displacement variables, the variables in the "strain" column matrix all have dimensions of strain; but the last of these variables, $\bar{\epsilon}$, is actually the axial force scaled by a factor. Differentiating the strain energy with respect to this variable does not produce a "force", but instead yields an implicit relation for the axial strain, a phenomenon which is characteristic of the Reissner-Hellinger variational principle. The ordering scheme is applied to the energy prior to undertaking these operations, thus guaranteeing the appropriate preservation of symmetry. Although formally negligible, the terms of cubic and higher degree in the 1-D strains are retained to improve modeling of bearingless rotors. These terms are simplified in that κ_x in those terms can be taken as ϕ'. This results in a simple expression for both the internal loads and the Jacobian.

3.5.1. Generalized internal forces

In order to define the generalized internal forces, first note that the 1-D generalized strain measures have the convenient property that derivatives of the 1-D strain energy function with respect to these measures gives the 1-D stress resultants which correspond to axial section force V_x, twisting moment M_x, and bending moments M_η and M_ζ. The derivative with respect to the "strain" $\bar{\epsilon}$ gives a quantity dubbed α, which has the dimensions of force, but may be regarded more properly as the residual of the inverse constitutive relation for the axial strain, and the subsequent application of a weighting function (i.e., $\delta\epsilon$) to this quantity will constitute the weak enforcement of the relation. The internal forces are, therefore,

$$\begin{aligned}
E_0A\bar{\epsilon} &= \frac{\partial\Phi}{\partial\epsilon_x},\\
M_x &= \frac{\partial\Phi}{\partial\kappa_x} = E_0D_0\bar{\epsilon} + \left(G_0J - \frac{E_0D_0^2}{A}\right)\kappa_x\\
&\quad + \left(E_0D_3 - E_0D_0e_{t\zeta}\right)\kappa_\eta + \left(-E_0D_2 + E_0D_0e_{t\eta}\right)\kappa_\zeta,\\
M_\eta &= \frac{\partial\Phi}{\partial\kappa_\eta} = E_0Ae_{t_\zeta}\bar{\epsilon} + \left(E_0D_3 - E_0D_0e_{t_\zeta}\right)\kappa_x\\
&\quad + \left(E_0I_\eta - E_0Ae_{t_\zeta}^2\right)\kappa_\eta + \left(E_0I_{\eta\zeta} + AE_0e_{t_\zeta}e_{t_\eta}\right)\kappa_\zeta,\\
M_\zeta &= \frac{\partial\Phi}{\partial\kappa_\zeta} = -E_0Ae_{t_\eta}\bar{\epsilon} + \left(-E_0D_2 + E_0D_0e_{t_\eta}\right)\kappa_x\\
&\quad + \left(E_0I_\zeta - E_0Ae_{t_\eta}^2\right)\kappa_\zeta + \left(E_0I_{\eta\zeta} + E_0Ae_{t_\zeta}e_{t_\eta}\right)\kappa_\eta,\\
\alpha &\equiv \frac{\partial\Phi}{\partial\bar{\epsilon}} = E_0A(\epsilon_x - \bar{\epsilon}) + E_0D_0\kappa_x + E_0Ae_{t_\zeta}\kappa_\eta - E_0Ae_{t_\eta}\kappa_\zeta.
\end{aligned} \tag{3.53}$$

These quantities correspond to the axial force, twisting moment, and bending moments in the deformed beam basis. They can be arranged in a column matrix $\{F\}$ so that

$$F_i = \frac{\partial\Phi}{\partial\gamma_i}, \tag{3.54}$$

where the subscript $i = 1,2,3,4,5$ refers to the set ϵ_x, κ_x, κ_η, κ_ζ, and $\bar{\epsilon}$. Note that γ is now defined as $\gamma = \{\epsilon_x, \kappa_x, \kappa_\eta, \kappa_\zeta, \bar{\epsilon}\}^\top$.

With anticipation of forming the Jacobian, a symmetric matrix $[K]$ is defined so that

$$K_{ij} = \frac{\partial^2 \Phi}{\partial \gamma_i \partial \gamma_j}. \tag{3.55}$$

Thus, $[K]$ is given by

$$[K] = \begin{bmatrix} 0 & 0 & 0 & 0 & E_0 A \\ 0 & G_0 J - \dfrac{E_0 D_0^2}{A} & E_0 D_3 - E_0 D_0 e_{t_\zeta} & -E_0 D_2 + E_0 D_0 e_{t_\eta} & E_0 D_0 \\ 0 & E_0 D_3 - E_0 D_0 e_{t_\zeta} & E_0 I_\eta - E_0 A e_{t_\zeta}^2 & E_0 I_{\eta\zeta} + A E_0 e_{t_\zeta} e_{t_\eta} & E_0 A e_{t_\zeta} \\ 0 & -E_0 D_2 + E_0 D_0 e_{t_\eta} & E_0 I_{\eta\zeta} + A E_0 e_{t_\zeta} e_{t_\eta} & E_0 I_\zeta - E_0 A e_{t_\eta}^2 & -E_0 A e_{t_\eta} \\ E_0 A & E_0 D_0 & E_0 A e_{t_\zeta} & -E_0 A e_{t_\eta} & -E_0 A \end{bmatrix}. \tag{3.56}$$

Both $\{F\}$ and $[K]$ are used below to obtain the generalized internal forces and the associated Jacobian.

To proceed with this development, it is necessary to carry out the variation of the strain energy with the 1-D strain measures written in terms of the variables of the analysis u, v, w, ϕ, $\bar{\epsilon}$ and their derivatives. First, the strain measures are written in terms of the displacement variables. Applying the ordering scheme and retaining terms to $O(\epsilon^2)$, one obtains

$$\begin{aligned} \epsilon_x &= \sqrt{(1+u')^2 + v'^2 + w'^2} - 1, \\ \kappa_x &= \phi' + v'' w', \\ \kappa_\eta &= v'' s_1 - w'' c_1, \\ \kappa_\zeta &= v'' c_1 + w'' s_1. \end{aligned} \tag{3.57}$$

The variation is now most easily done using index notation and the chain rule. Introducing the column matrix

$$\{z\} = \{u \quad v \quad w \quad \phi \quad u' \quad v' \quad w' \quad \phi' \quad u'' \quad v'' \quad w'' \quad \phi'' \quad \bar{\epsilon}\}^\top, \tag{3.58}$$

with indices which vary from 1–13, and letting all repeated indices be summed over their range, one can express the first variation of Φ as

$$\delta\Phi = \frac{\partial \Phi}{\partial \gamma_i} \frac{\partial \gamma_i}{\partial z_j} \delta z_j = F_i R_{ij} \delta z_j = \delta\{z\}^\top [R]^\top \{F\}, \tag{3.59}$$

where $[R]$ and $\{F\}$ are given by

$$[R] = \begin{bmatrix} 0 & 0 & 0 & 0 & \dfrac{(1+u')}{\epsilon_x + 1} & \dfrac{v'}{\epsilon_x + 1} & \dfrac{w'}{\epsilon_x + 1} & 0 & 0 & 0 & 0 & 0 & 0 \\ 0 & 0 & 0 & 0 & 0 & 0 & v'' & 1 & 0 & w' & 0 & 0 & 0 \\ 0 & 0 & 0 & \kappa_\zeta & 0 & 0 & 0 & 0 & 0 & s_1 & -c_1 & 0 & 0 \\ 0 & 0 & 0 & -\kappa_\eta & 0 & 0 & 0 & 0 & 0 & c_1 & s_1 & 0 & 0 \\ 0 & 0 & 0 & 0 & 0 & 0 & 0 & 0 & 0 & 0 & 0 & 0 & 1 \end{bmatrix}, \tag{3.60}$$

$$\{F\} = \begin{Bmatrix} E_0 A \bar{\epsilon} \\ M_x \\ M_\eta \\ M_\zeta \\ \alpha \end{Bmatrix}.$$

It is now easily seen that the column matrix of generalized forces corresponding to $\{z\}$ as defined above is

$$\{f\} = [R]^{\top}\{F\}. \tag{3.61}$$

The column matrix $\{f\}$ can be written explicitly as

$$\{f\} = \begin{Bmatrix} 0 \\ 0 \\ 0 \\ M_\eta \kappa_\zeta - M_\zeta \kappa_\eta \\ \dfrac{E_0 A \bar{\epsilon}(1+u')}{\epsilon_x + 1} \\ \dfrac{E_0 A \bar{\epsilon} v'}{\epsilon_x + 1} \\ \dfrac{E_0 A \bar{\epsilon} w'}{\epsilon_x + 1} + v'' M_x \\ M_x \\ 0 \\ w' M_x + M_\zeta c_1 + M_\eta s_1 \\ M_\zeta s_1 - M_\eta c_1 \\ 0 \\ E_0 A(\epsilon_x - \bar{\epsilon}) + E_0 D_0 \kappa_x + E_0 A e_{t_\zeta} \kappa_\eta - E_0 A e_{t_\eta} \kappa_\zeta \end{Bmatrix}. \tag{3.62}$$

The contribution of the internal forces is then expressible as

$$\delta U = \int_0^\ell \delta\{z\}^{\top} f \, dx. \tag{3.63}$$

3.5.2. Jacobian

The contribution of these terms to the perturbation equations is obtained from forming the Jacobian. This is like taking one more variation, resulting in

$$\Delta\delta\Phi = \delta z_i \left(R_{ki} K_{kl} R_{lj} + \frac{\partial^2 \gamma_k}{\partial z_i \partial z_j} F_k \right) \Delta z_j. \tag{3.64}$$

Thus, the contribution can be written in matrix form as

$$\Delta\delta U = \int_0^\ell \delta\{z\}^{\top} ([K_1] + [K_2]) \, \Delta\{z\} \, dx, \tag{3.65}$$

where $[K_1]$ is given by

$$[K_1] = [R]^{\top}[K][R], \tag{3.66}$$

and $[K_2]$ is

$$[K_2] = \begin{bmatrix}
0 & 0 & 0 & 0 & 0 & 0 & 0 & 0 & 0 & 0 & 0 & 0 \\
0 & 0 & 0 & 0 & 0 & 0 & 0 & 0 & 0 & 0 & 0 & 0 \\
0 & 0 & 0 & 0 & 0 & 0 & 0 & 0 & 0 & 0 & 0 & 0 \\
0 & 0 & 0 & -(M_\eta \kappa_\eta + M_\zeta \kappa_\zeta) & 0 & 0 & 0 & 0 & 0 & M_\eta c_1 - M_\zeta s_1 & M_\eta s_1 + M_\zeta c_1 & 0 & 0 \\
0 & 0 & 0 & 0 & 0 & 0 & 0 & 0 & 0 & 0 & 0 & 0 & 0 \\
0 & 0 & 0 & 0 & 0 & E_0 A \bar{\epsilon} & 0 & 0 & 0 & 0 & 0 & 0 & 0 \\
0 & 0 & 0 & 0 & 0 & 0 & E_0 A \bar{\epsilon} & 0 & 0 & M_x & 0 & 0 & 0 \\
0 & 0 & 0 & 0 & 0 & 0 & 0 & 0 & 0 & 0 & 0 & 0 & 0 \\
0 & 0 & 0 & 0 & 0 & 0 & 0 & 0 & 0 & 0 & 0 & 0 & 0 \\
0 & 0 & 0 & M_\eta c_1 - M_\zeta s_1 & 0 & 0 & M_x & 0 & 0 & 0 & 0 & 0 & 0 \\
0 & 0 & 0 & M_\eta s_1 + M_\zeta c_1 & 0 & 0 & 0 & 0 & 0 & 0 & 0 & 0 & 0 \\
0 & 0 & 0 & 0 & 0 & 0 & 0 & 0 & 0 & 0 & 0 & 0 & 0 \\
0 & 0 & 0 & 0 & 0 & 0 & 0 & 0 & 0 & 0 & 0 & 0 & 0
\end{bmatrix}. \tag{3.67}$$

Thus, the strain energy contribution to the Jacobian is given *explicitly* in terms of $[K_1] + [K_2]$. Only the nonzero elements of $[K_1]$ should be calculated.

4. MODAL REDUCTION WITH MIXED ELEMENTS

If mixed elements are employed, it may seem straightforward to recover the finite-element displacements from modal coordinates by employing the usual modal reduction relation

$$\{q\} = [\Phi]\{\alpha\}, \tag{4.68}$$

where $[\Phi]$ is the modal matrix, α is a vector of modal coordinates, and $\{q\}$ are the finite-element degrees of freedom, in which $\{q\}$ includes the axial force degrees of freedom. However, using this approach implicitly retains a linear relation between the axial forces and displacements, which is not generally correct. This problem may be dealt with by retaining the axial forces as *independent* degrees of freedom. To accomplish this, each eigenvector is written as follows:

$$\{\phi_i\} = \begin{Bmatrix} \phi_d \\ \phi_f \end{Bmatrix}, \tag{4.69}$$

where $\{\phi_i\}$ is the i^{th} modal vector, $\{\phi_d\}$ is the displacement part of the eigenmode, and $\{\phi_f\}$ is the force part of the eigenmode. When modal reduction is performed, $\{\phi_i\}$ is split into two vectors containing the force and displacement parts separately:

$$\{\phi_i\} \mapsto [\phi_1 \mid \phi_2] = \begin{bmatrix} \phi_d & 0 \\ 0 & \phi_f \end{bmatrix}. \tag{4.70}$$

This approach permits sufficient decoupling of the axial displacements and forces to enable the accurate calculation of each. It has the drawback of requiring that additional generalized coordinates be added to the analysis, but in practice, only one or two of these are needed.

5. COMPUTATIONAL EXAMPLES OF MODAL REDUCTION WITH MIXED ELEMENTS

The modal reduction accuracy of mixed elements will now be studied using the examples examined earlier during the discussion of the axial displacement variable.

The first example is the flap frequencies of the articulated blade. Plots of the first two flap frequencies versus the number of axial modes are shown in Figure 6. In contrast to the corresponding results seen in Figure 2 for the displacement element, only a single axial mode—but actually, two generalized coordinates—are required to match the finite-element results accurately.

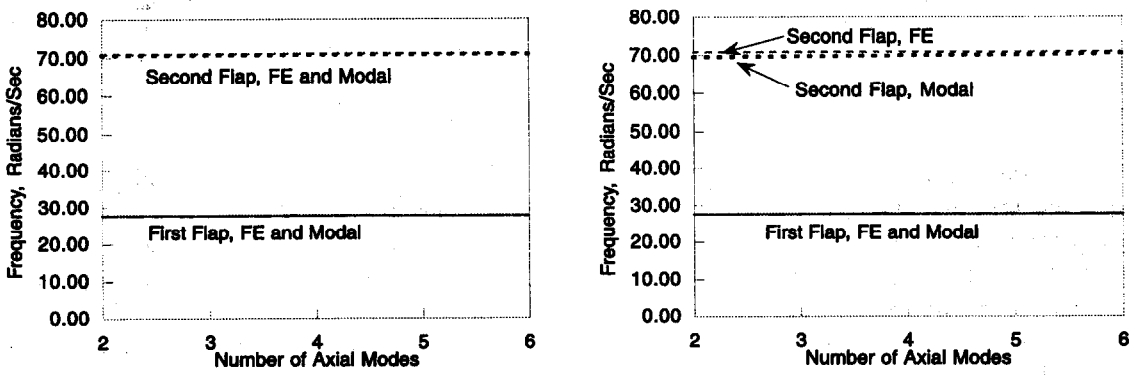

(a) Four degrees coning angle.

(b) Eight degrees coning angle.

Figure 6. Articulated blade flap frequencies: mixed elements.

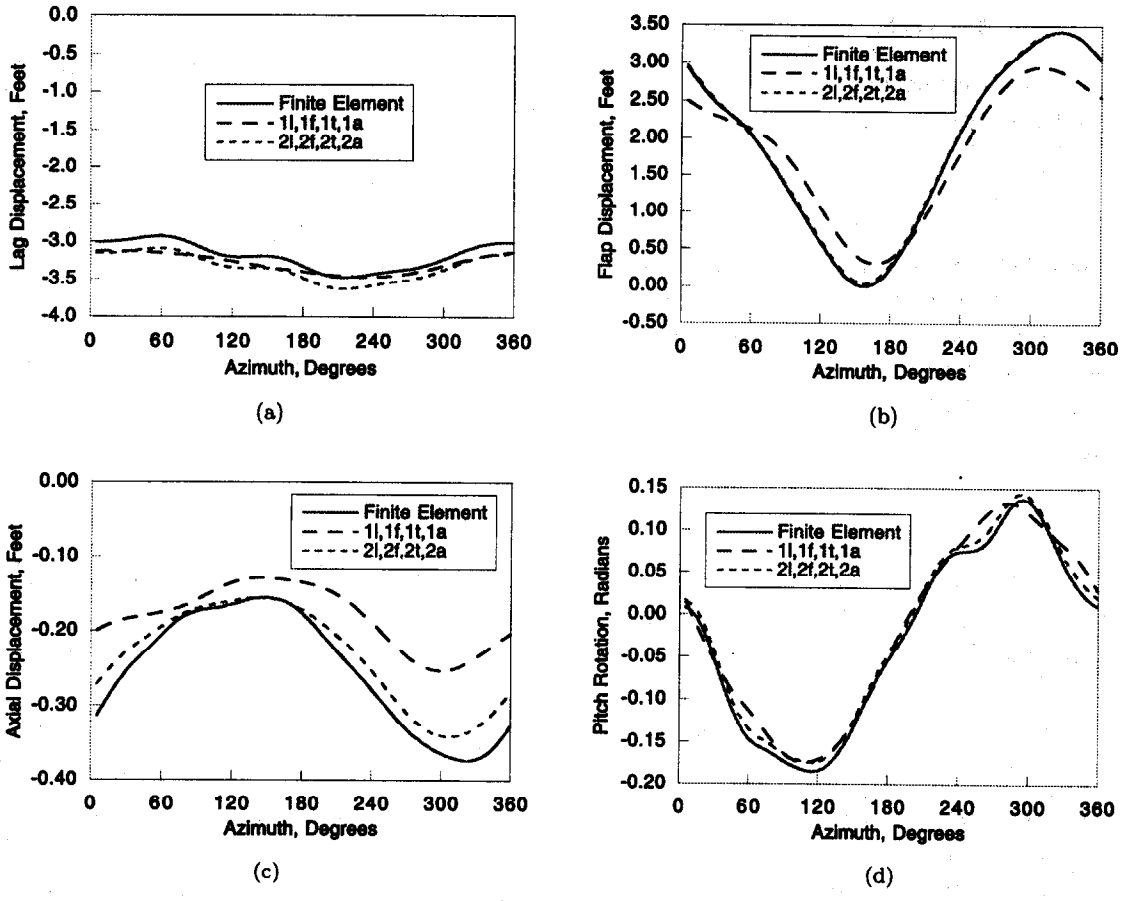

Figure 7. Articulated blade tip deflections: mixed elements.

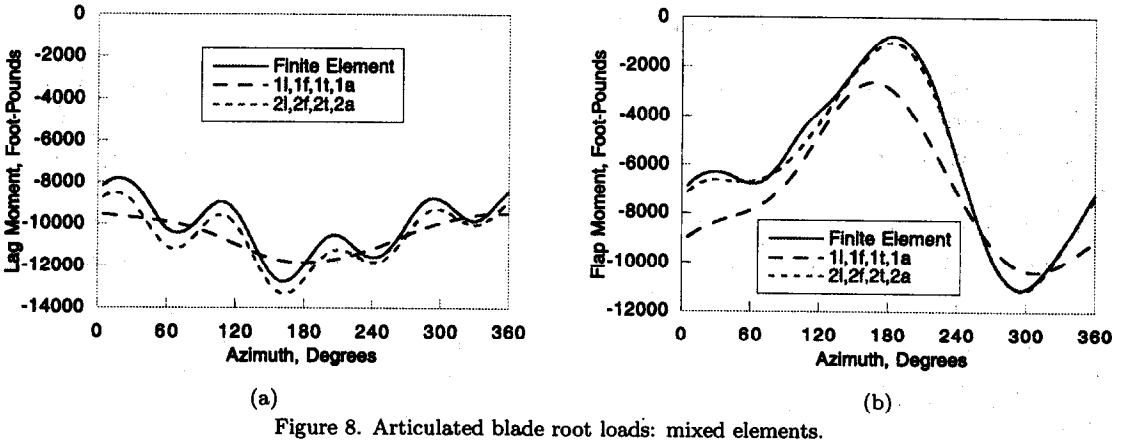

Figure 8. Articulated blade root loads: mixed elements.

Periodic solutions for finite-element and modal bases compared in Figure 7 for blade tip displacements, and in Figure 8 for blade root loads. It may be seen that there is a dramatic improvement in how the modal solutions approximate blade tip displacements when compared with the corresponding results for the displacement elements (Figure 3). The axial displacement is not approximated quite as well as the other displacements, probably because of the nonlinearity of the axial foreshortening effect. However, the primary interest in the axial displacement is its impact on lag moments through the Coriolis effect, but as may be seen in Figure 8, the modal approximations of the root lag moments is quite good, which suggests that the modal approximation of the axial displacement is satisfactory for practical purposes.

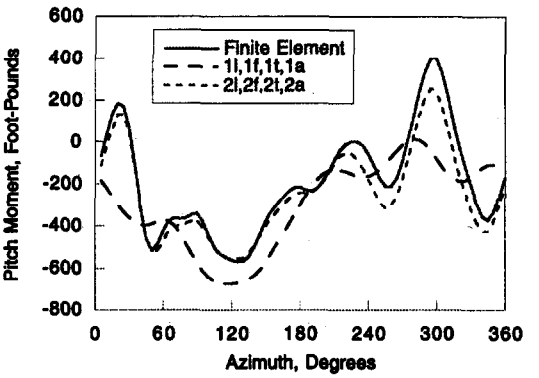

(c)

Figure 8. (cont.).

6. CONCLUSIONS

The modal reduction accuracy of several blade analyses is examined by applying the analyses to the Hodges-Dowell blade equations, specialized to coupled flap-axial motions. It is shown that representing the axial motions using the axial displacement variable simplifies model discretization, but suffers from poor modal reduction accuracy owing to numerical ill conditioning and nonlinearities in the formulation. Qualititative arguments, buttressed by reports of the success of the axial elongation variable, suggest that use of the axial force as a variable should significantly improve modal reduction accuracy, but any improvement would come at the expense of reduced modeling flexibility. A mixed element is presented as an alternative that seeks to combine the advantages of the other two methods by using both displacements and forces to represent axial motions. The derivation of the complete, mixed element is then described, and the modifications to the usual modal combination algorithm to account for the axial force degrees of freedom are presented. Finally, the good modal reduction accuracy of the mixed element is demonstrated by applying it to the analysis of an articulated blade model.

APPENDIX: MIXED ELEMENT INERTIA TERMS

The inertia terms of the mixed element are derived in this Appendix. These terms are obtained by forming the integral of the virtual work due to inertial loads from the time integral of the variation of the kinetic energy, and then integrating by parts. First, expressions are written for the velocity of an arbitrary point on the beam reference line and the angular velocity of the deformed beam cross-section, assuming that the warping of the section is ignored for the purpose of determination of the kinetic energy. Next, the kinetic energy is written based on the geometrically exact formulation of [4], using the cross-sectional integrals defined therein. Finally, the contribution to the final equations of motion from inertial and gravitational forces is determined by a series of operations which include variation with respect to all unknown coordinate functions, integration by parts in the time domain, and application of the ordering scheme. The ordering scheme need not be invoked until the last step.

A.1. Kinematics

For the purpose of writing the kinetic energy in compact form, the column matrix $\{v_E^{A'I}\}$ is written as

$$\left\{v_E^{A'I}\right\} = \{v_E^{EI}\} + \left\{\dot{r}_E^{A'E}\right\} + \left[\widetilde{\omega_E^{EI}}\right]\left\{r_E^{A'E}\right\}, \tag{A.71}$$

where $\{v_E^{EI}\}$ is the column matrix, the elements of which are measure numbers of $\mathbf{v}^{EI}$, $\{\omega_E^{EI}\}$ is the column matrix, the elements of which are measure numbers of ω^{EI}, and (neglecting warping

effects)

$$\left\{r_E^{A'E}\right\} = \begin{Bmatrix} x+u \\ v \\ w \end{Bmatrix}. \tag{A.72}$$

The column matrix $\{\omega_{S'}^{S'I}\}$ contains the measure numbers of the angular velocity of the deformed beam cross-sectional frame $\omega^{S'I}$ in the deformed beam basis. An approximation consistent with the ordering scheme is given by

$$\left\{\omega_{S'}^{S'I}\right\} = \begin{bmatrix} 1 & 0 & w' \\ 0 & c_1 & s_1 \\ 0 & -s_1 & c_1 \end{bmatrix} \begin{Bmatrix} \dot{\phi} \\ -\dot{w}' \\ \dot{v}' \end{Bmatrix} + \left[T^{S'E}\right] \left\{\omega_E^{EI}\right\}. \tag{A.73}$$

Finally, consider the virtual rotation of S' in I. Since the motion of E is prescribed in I, this is the same as the virtual rotation of S' in E, denoted by $\overline{\delta\theta}^{S'E}$. From [10], this vector can be written as

$$\overline{\delta\theta}^{S'E} = \overline{\delta\theta}_{S'_i}^{S'E} \mathbf{b}_i^{S'}, \tag{A.74}$$

where, within the accuracy of the ordering scheme, the column matrix containing these elements can be written as

$$\left\{\overline{\delta\theta}_{S'}^{S'E}\right\} = \begin{bmatrix} 1 & 0 & w' \\ 0 & c_1 & s_1 \\ 0 & -s_1 & c_1 \end{bmatrix} \begin{Bmatrix} \delta\phi \\ -\delta w' \\ \delta v' \end{Bmatrix}. \tag{A.75}$$

A.2. Kinetic Energy Expression

The kinetic energy can now be written as

$$K = \frac{1}{2}\int_0^\ell \times \left[m\left\{v_E^{A'I}\right\}^{\mathrm{T}}\left\{v_E^{A'I}\right\} + 2m\left\{\omega_{S'}^{S'I}\right\}^{\mathrm{T}}[\tilde{e}]\left[T^{S'E}\right]\left\{v_E^{A'I}\right\} + \left\{\omega_{S'}^{S'I}\right\}^{t} op\,[I]\left\{\omega_{S'}^{S'I}\right\}\right] dx, \tag{A.76}$$

where $\{e\}$ is given by

$$\{e\} = \begin{Bmatrix} 0 \\ e_{m_\eta} \\ e_{m_\zeta} \end{Bmatrix}. \tag{A.77}$$

$e_{m_\eta} = \langle\rho\eta\rangle$, $e_{m_\zeta} = \langle\rho\zeta\rangle$, $[I]$ is the sectional inertia matrix given by

$$[I] = \begin{bmatrix} i_\eta + i_\zeta & 0 & 0 \\ 0 & i_\eta & i_{\eta\zeta} \\ 0 & i_{\eta\zeta} & i_\zeta \end{bmatrix}, \tag{A.78}$$

and $i_\eta = \langle\rho\zeta^2\rangle$, $i_\zeta = \langle\rho\eta^2\rangle$, and $i_{\eta\zeta} = -\langle\rho\zeta\eta\rangle$. This is a geometrically exact expression for the kinetic energy, provided that all vector quantities are written exactly. (Note that the radii of gyration can be obtained from $k_{m\eta} = \sqrt{i_\zeta/m}$ and $k_{m\zeta} = \sqrt{i_\eta/m}$.) The result for the virtual work of body forces is of the form

$$\delta W_b = \delta W_{b0} + \delta W_{b1} + \delta W_{b2}, \tag{A.79}$$

where the subscript b refers to these as body force terms, and the subscripts 0, 1, and 2 refer to the zeroth, first, and second moment terms, respectively. Below, the first term (the zeroth moment term of K) is written exactly. The second term (the first moment) and the third term (the second moment) are approximated and have been carried out via computer-aided symbolic manipulation based on the above approximation of $\{\omega_{S'}^{S'I}\}$.

A.3. Exact Term

When δK is substituted into Hamilton's principle, the first term must be integrated from fixed times t_1 and t_2. After doing this, integrating by parts in time, and setting $\delta\{r_E^{A'E}\}$ equal to zero at $t = t_1$ and $t = t_2$, one obtains the contribution of this term to the virtual work of the inertial forces

$$\delta W_{b0} = -\int_0^\ell m\delta\left\{r_E^{A'E}\right\}^\top \times\left\{\left\{a_E^{EI}\right\}+\left\{r_E^{\ddot{A}'E}\right\}+2\left[\widetilde{\omega_E^{EI}}\right]\left\{\dot{r}_E^{A'E}\right\}+\left[\left[\widetilde{\omega_E^{EI}}\right]\left[\widetilde{\omega_E^{EI}}\right]+\left[\dot{\widetilde{\omega_E^{EI}}}\right]\right]\left\{r_E^{A'E}\right\}\right\} dx. \tag{A.80}$$

This can be written as four terms, three on the left-hand side of the equations of motion (the signs are changed on these terms to reflect the change from right to left), and one on the right-hand side. The left-hand-side contributions are to the mass matrix

$$\int_0^\ell m\begin{Bmatrix}\delta u\\ \delta v\\ \delta w\end{Bmatrix}^\top\begin{Bmatrix}\ddot{u}\\ \ddot{v}\\ \ddot{w}\end{Bmatrix} dx, \tag{A.81}$$

the gyroscopic matrix (which is nondissipative)

$$2\int_0^\ell m\begin{Bmatrix}\delta u\\ \delta v\\ \delta w\end{Bmatrix}^\top\left[\widetilde{\omega_E^{EI}}\right]\begin{Bmatrix}\dot{u}\\ \dot{v}\\ \dot{w}\end{Bmatrix} dx, \tag{A.82}$$

and the stiffness matrix

$$\int_0^\ell m\begin{Bmatrix}\delta u\\ \delta v\\ \delta w\end{Bmatrix}^\top\left[\left[\widetilde{\omega_E^{EI}}\right]\left[\widetilde{\omega_E^{EI}}\right]+\left[\dot{\widetilde{\omega_E^{EI}}}\right]\right]\begin{Bmatrix}u\\ v\\ w\end{Bmatrix} dx, \tag{A.83}$$

where the associated rotation matrices are

$$\left[\widetilde{\omega_E^{EI}}\right]\left[\widetilde{\omega_E^{EI}}\right]=\begin{bmatrix}-(\omega_2^2+\omega_3^2) & \omega_1\omega_2 & \omega_1\omega_3\\ \omega_1\omega_2 & -(\omega_1^2+\omega_3^2) & \omega_2\omega_3\\ \omega_1\omega_3 & \omega_2\omega_3 & -(\omega_1^2+\omega_2^2)\end{bmatrix} \tag{A.84}$$

and

$$\left[\dot{\widetilde{\omega_E^{EI}}}\right]=\begin{bmatrix}0 & -\dot{\omega}_3 & \dot{\omega}_2\\ \dot{\omega}_3 & 0 & -\dot{\omega}_1\\ -\dot{\omega}_2 & \dot{\omega}_1 & 0\end{bmatrix}. \tag{A.85}$$

All the remaining terms contribute to the residual on the right-hand side of the equations. This contribution is

$$-\int_0^\ell m\begin{Bmatrix}\delta u\\ \delta v\\ \delta w\end{Bmatrix}^\top\left\{\left\{a_E^{EI}\right\}+x\left[\left[\widetilde{\omega_E^{EI}}\right]\left[\widetilde{\omega_E^{EI}}\right]+\left[\dot{\widetilde{\omega_E^{EI}}}\right]\right]\begin{Bmatrix}1\\ 0\\ 0\end{Bmatrix}\right\} dx. \tag{A.86}$$

Gravity can be treated with the inertial forces just by replacing $\{a_E^{EI}\}$ with $\{a_E^{EI}\}-\{g_E\}$ where $\{g_E\}$ is the column matrix which contains the measure numbers of the gravity vector in E basis.

A.4. First Moment Term

The second term in the kinetic energy contains the contributions from the offset of the beam reference axis and the sectional mass centroid. If sectional analysis codes are used, the reference line can be input as the mass centroid which removes all these terms from the equations.

Taking the variation and integrating over time, one obtains

$$\int_{t_1}^{t_2} \delta K\, dt = \int_{t_1}^{t_2} \int_0^{\ell} \left(m\delta \left\{\omega_{S'}^{S'I}\right\}^{\top} [\tilde{e}] \left[T^{S'E}\right] \left\{v_E^{A'I}\right\} + m \left\{\omega_{S'}^{S'I}\right\}^{\top} [\tilde{e}]\, \delta \left[T^{S'E}\right] \left\{v_E^{A'I}\right\} \right.$$
$$\left. + m \left\{\omega_{S'}^{S'I}\right\}^{\top} [\tilde{e}] \left[T^{S'E}\right] \delta \left\{v_E^{A'I}\right\} \right) dx\, dt + \cdots . \tag{A.87}$$

The variation of the angular velocity can be written in terms of the virtual rotation $\{\overline{\delta\theta}_{S'}^{S'E}\}$ according to [4] as

$$\delta \left\{\omega_{S'}^{S'I}\right\} = \left\{\dot{\overline{\delta\theta}}_{S'}^{S'E}\right\} + \left[\widetilde{\omega_{S'}^{S'I}}\right] \left\{\overline{\delta\theta}_{S'}^{S'E}\right\}. \tag{A.88}$$

Also, the variation of $[T^{S'E}]$ can be expressed in terms of the virtual rotation as

$$\delta \left[T^{S'E}\right] = - \left[\widetilde{\overline{\delta\theta}_{S'}^{S'E}}\right] \left[T^{S'E}\right]. \tag{A.89}$$

With these substitutions, the contribution to the equations of motion can be shown to be in these two terms:

$$\delta K = - \int_0^{\ell} m \left(\left\{\overline{\delta\theta}_{S'}^{S'E}\right\}^{\top} [\tilde{e}] \left[T^{S'E}\right] \left\{ \left\{a_E^{EI}\right\} + \left\{r_E^{\ddot{A}'E}\right\} \right.\right.$$
$$+2 \left[\widetilde{\omega_E^{EI}}\right] \left\{r_E^{\dot{A}'E}\right\} + \left[\left[\widetilde{\omega_E^{EI}}\right] \left[\widetilde{\omega_E^{EI}}\right] + \left[\dot{\widetilde{\omega_E^{EI}}}\right] \right] \left\{r_E^{A'E}\right\} \Big\} \tag{A.90}$$
$$\left. + \delta \left\{r_E^{A'E}\right\}^{\top} \left[T^{S'E}\right]^{\top} \left[\left[\widetilde{\omega_{S'}^{S'I}}\right] \left[\widetilde{\omega_{S'}^{S'I}}\right] + \left[\dot{\widetilde{\omega_{S'}^{S'I}}}\right] \right] \{e\} \right) dx + \cdots .$$

This expression is geometrically exact. However, in the present theory $[T^{S'E}]$, $\{\omega_{S'}^{S'I}\}$, and $\{\overline{\delta\theta}_{S'}^{S'E}\}$ are approximated as in equations (3.37), (A.73), and (A.75), respectively. The offset quantities are assumed to be $O(\epsilon^2)$. Thus, the terms multiplied by the offsets need only be retained to $O(\epsilon)$.

The above operations result in the contribution of the first moment terms to the virtual work of the inertial force terms on the right-hand side. These can be simplified by introducing

$$e_{m_y} = c_1 e_{m_\eta} - s_1 e_{m_\zeta}, \qquad e_{m_z} = s_1 e_{m_\eta} + c_1 e_{m_\zeta}, \tag{A.91}$$

so that the generalized body force contributions from the first moment terms are

$$\delta W_{b1} = \int_0^{\ell} \delta v \left[e_{m_y} \left({\omega_1}^2 + {\omega_3}^2 + 2\omega_1\dot{\phi} + \dot{\phi}^2 \right) - e_{m_z} \left(\omega_2\omega_3 - \dot{\omega}_1 - \ddot{\phi} \right) \right] dx$$
$$- \int_0^{\ell} \delta w \left[e_{m_y} \left(\omega_2\omega_3 + \dot{\omega}_1 + \ddot{\phi} \right) - e_{m_z} \left({\omega_1}^2 + {\omega_2}^2 + 2\omega_1\dot{\phi} + \dot{\phi}^2 \right) \right] dx$$
$$- \int_0^{\ell} \delta\phi \left\{ e_{m_y} \left[A_3 - \left({\omega_1}^2 + {\omega_2}^2 \right) w - \left(A_1 - x{\omega_2}^2 - x{\omega_3}^2 \right) w' \right.\right.$$
$$+ v \left(\omega_2\omega_3 + \dot{\omega}_1\right) + x \left(\omega_1\omega_3 - \dot{\omega}_2\right) + 2\omega_1\dot{v} + \ddot{w} \Big] \tag{A.92}$$
$$+ e_{m_z} \left[-A_2 + \left({\omega_1}^2 + {\omega_3}^2 \right) v + \left(A_1 - x{\omega_2}^2 - x{\omega_3}^2 \right) v' \right.$$
$$\left.\left. + w \left(-\omega_2\omega_3 + \dot{\omega}_1\right) - x \left(\omega_1\omega_2 + \dot{\omega}_3\right) + 2\omega_1\dot{w} - \ddot{v} \right] \right\} dx$$
$$+ \int_0^{\ell} \delta w' e_{m_z} \left[A_1 - x \left({\omega_2}^2 + {\omega_3}^2 \right) \right] dx$$
$$+ \int_0^{\ell} \delta v' e_{m_y} \left[A_1 - x \left({\omega_2}^2 + {\omega_3}^2 \right) \right] dx.$$

Note that in this expression there are no linear terms.

The first moment term yields a total of 17 terms in the perturbed equations of motion, the signs of which are changed to reflect their being on the left-hand side of the equations of motion. In virtual work form, the four "mass matrix" terms are

$$\begin{aligned} -\Delta\delta W_{b1} = &-\int_0^\ell \delta v\, m e_{m_x} \Delta\ddot{\phi}\, dx \\ &+\int_0^\ell \delta w\, m e_{m_y} \Delta\ddot{\phi}\, dx \\ &-\int_0^\ell \delta\phi\, m e_{m_x} \Delta\ddot{v}\, dx \\ &+\int_0^\ell \delta\phi\, m e_{m_y} \Delta\ddot{w}\, dx + \cdots . \end{aligned} \tag{A.93}$$

The four "gyroscopic matrix" terms are

$$\begin{aligned} -\Delta\delta W_{b1} = &-2\int_0^\ell \delta v\, m e_{m_y} \left(\omega_1 + \dot{\phi}\right) \Delta\dot{\phi}\, dx \\ &-2\int_0^\ell \delta w\, m e_{m_x} \left(\omega_1 + \dot{\phi}\right) \Delta\dot{\phi}\, dx \\ &+2\omega_1 \int_0^\ell \delta\phi\, m e_{m_y} \Delta\dot{v}\, dx \\ &+2\omega_1 \int_0^\ell \delta\phi\, m e_{m_x} \Delta\dot{w}\, dx + \cdots . \end{aligned} \tag{A.94}$$

The nine terms contributing to the Jacobian are

$$\begin{aligned} -\Delta\delta W_{b1} = &\int_0^\ell \delta v\, m \left[e_{m_y}\left(\omega_2\omega_3 - \dot{\omega}_1 - \ddot{\phi}\right) + e_{m_x}\left({\omega_1}^2 + {\omega_3}^2 + 2\omega_1\dot{\phi} + \dot{\phi}^2\right)\right] \Delta\phi\, dx \\ &-\int_0^\ell \delta w\, m \left[e_{m_y}\left({\omega_1}^2 + {\omega_2}^2 + 2\omega_1\dot{\phi} + \dot{\phi}^2\right) + e_{m_x}\left(\omega_2\omega_3 + \dot{\omega}_1 + \ddot{\phi}\right)\right] \Delta\phi\, dx \\ &+\int_0^\ell \delta\phi\, m \left[e_{m_y}\left(\omega_2\omega_3 + \dot{\omega}_1\right) + e_{m_x}\left({\omega_1}^2 + {\omega_3}^2\right)\right] \Delta v\, dx \\ &-\int_0^\ell \delta\phi\, m \left[e_{m_y}\left({\omega_1}^2 + {\omega_2}^2\right) + e_{m_x}\left(\omega_2\omega_3 - \dot{\omega}_1\right)\right] \Delta w\, dx \\ &+\int_0^\ell \delta\phi\, m \left\{e_{m_y}\left[-A_2 - x\omega_1\omega_2 + {\omega_1}^2 v + {\omega_3}^2 v - \omega_2\omega_3 w\right.\right. \\ &\quad \left. + w\dot{\omega}_1 - x\dot{\omega}_3 + 2\omega_1\dot{w} - \ddot{v} + \left(A_1 - x{\omega_2}^2 - x{\omega_3}^2\right) v'\right] \\ &\quad + e_{m_x}\left[-A_3 - x\omega_1\omega_3 - \omega_2\omega_3 v + {\omega_1}^2 w + {\omega_2}^2 w\right. \\ &\left.\left. - v\dot{\omega}_1 + x\dot{\omega}_2 - 2\omega_1\dot{v} - \ddot{w} + \left(A_1 - x{\omega_2}^2 - x{\omega_3}^2\right) w'\right]\right\} \Delta\phi\, dx \\ &-\int_0^\ell \delta w'\, m e_{m_y} \left[A_1 - x\left({\omega_2}^2 + {\omega_3}^2\right)\right] \Delta\phi\, dx \\ &+\int_0^\ell \delta v'\, m e_{m_x} \left[A_1 - x\left({\omega_2}^2 + {\omega_3}^2\right)\right] \Delta\phi\, dx \\ &-\int_0^\ell \delta\phi\, m e_{m_y} \left[A_1 - x\left({\omega_2}^2 + {\omega_3}^2\right)\right] \Delta w'\, dx \\ &+\int_0^\ell \delta\phi\, m e_{m_x} \left[A_1 - x\left({\omega_2}^2 + {\omega_3}^2\right)\right] \Delta v'\, dx + \cdots . \end{aligned} \tag{A.95}$$

A.5. Second Moment Term

The third term in the kinetic energy contains the contributions from the sectional inertia matrix $[I]$. Taking the variation of this term and integrating over time yields

$$\int_{t_1}^{t_2} \delta K \, dt = \int_{t_1}^{t_2} \int_0^{\ell} \delta \left\{ \omega_{S'}^{S'I} \right\}^{\top} [I] \left\{ \omega_{S'}^{S'I} \right\} dx \, dt + \cdots . \tag{A.96}$$

Substituting equation (A.88), integrating by parts, and setting $\{\overline{\delta\theta}_{S;}^{S'E'}\}$ equal to zero at $t = t_1$ and $t = t_2$, one obtains the contribution of these terms to the equations of motion

$$\delta K = - \int_0^{\ell} \left\{ \overline{\delta\theta}_{S'}^{S'E} \right\}^{\top} \left[[I] \left\{ \dot{\omega}_{S'}^{S'I} \right\} + \left[\widetilde{\omega_{S'}^{S'I}} \right] [I] \left\{ \omega_{S'}^{S'I} \right\} \right] dx + \cdots . \tag{A.97}$$

The sectional mass moments of inertia can be regarded as $O(mR^2\epsilon^3)$; thus, the terms multiplied by them need only be retained to $O(1)$. To this order, there are only two second moment terms. The first is a linear term in the mass matrix, the sign of which is changed to reflect its being on the left-hand side,

$$-\delta W_{b2} = \int_o^{\ell} \delta\phi \, (i_\eta + i_\zeta) \, \ddot{\phi} \, dx + \cdots . \tag{A.98}$$

The second is the residual, in which there is only a nonlinear torsional moment term, given by

$$\begin{aligned} \delta W_{b2} = \int_o^{\ell} \delta\phi \left\{ (i_\eta - i_\zeta) \left[\left({c_1}^2 - {s_1}^2 \right) \omega_2 \omega_3 - \left({\omega_2}^2 - {\omega_3}^2 \right) s_1 c_1 \right] \right. \\ \left. - i_{\eta\zeta} \left[4 c_1 s_1 \omega_2 \omega_3 + \left({c_1}^2 - {s_1}^2 \right) \left({\omega_2}^2 - {\omega_3}^2 \right) \right] - (i_\eta + i_\zeta) \dot{\omega}_1 \right\} dx + \cdots . \end{aligned} \tag{A.99}$$

Note that there are no linear terms in this expression. (The one linear term which would have been present is in the mass matrix and not repeated in the residual.) The Jacobian of this expression only contains the one term

$$\begin{aligned} -\Delta\delta W_{b2} = \int_o^{\ell} \delta\phi \left\{ \left[\left({c_1}^2 - {s_1}^2 \right) (i_\eta - i_\zeta) - 4 s_1 c_1 i_{\eta\zeta} \right] \left(\omega_2^2 - \omega_3^2 \right) \right. \\ \left. + 4 \left[\left({c_1}^2 - {s_1}^2 \right) i_{\eta\zeta} + s_1 c_1 \, (i_\eta - i_\zeta) \right] \omega_2 \omega_3 \right\} \Delta\phi \, dx. \end{aligned} \tag{A.100}$$

This part of the formulation can be extended, if necessary, to the case in which the sectional mass moments of inertia are $O(mR^2\epsilon^2)$. The contribution of these neglected terms, however, is believed to be negligible for most rotor blades.

REFERENCES

1. E.C. Smith, Aeroelastic response and aeromechanical stability of helicopters with elastically coupled composite rotor blades UM-AERO 92-15 (July 1992).
2. T.R. Kane, R.R. Ryan and A.K. Banerjee, Dynamics of a cantilever beam attached to a moving base, *AIAA Journal of Guidance, Control and Dynamics* **10** (March/April 1987).
3. S.W. Shaw and C. Pierre, Normal modes for non-linear vibratory systems, *Journal of Sound and Vibration* **164** (1) (1993).
4. D.H. Hodges, A mixed variational formulation based on exact intrinsic equations for dynamics of moving beams, *International Journal of Solids and Structures* **20** (11) (1990).
5. O.A. Bauchau and C. Guernsey, On the choice of appropriate bases for nonlinear dynamic analyses, *Journal of the American Helicopter Society* **38** (4) (October 1993).
6. A.K. Noor and J.M. Peters, Reduced basis technique for nonlinear analysis of structures, *AIAA Jounal* **19** (4) (1980).
7. D.H. Hodges and E.H. Dowell, Nonlinear equations of motion for the elastic bending and torsion of twisted nonuniform rotor blades, NASA TN D-7818.
8. W. Johnson, *Helicopter Theory*, Princeton University Press, (1980).
9. J.S. Przemieniecki, *Theory of Matrix Structural Analysis*, McGraw-Hill, (1968).

10. D.W. Hodges, R.A. Ormiston and D.A. Peters, On the nonlinear deformation geometry of Euler-Bernoulli beams, NASA Technical Paper 1566 (April 1980).
11. B.A. Szabo and I. Babuska, *Finite Element Analysis*, John Wiley & Sons, (1991).
12. 2GCHAS Theory Manual, USAATCOM Technical Memorandum 93-A-004 (1993).
13. T.R. Kane, P.W. Likins and D.A. Levinson, *Spacecraft Dynamics*, McGraw-Hill, (1983).
14. D.H. Hodges, Torsion of pretwisted beams due to axial loading, *ASME Journal of Applied Mechanics* **47** (1980).
15. V.L. Berdichevsky, Equations of the theory of anisotropic inhomogeneous rods, *Soviet Physics Doklady* **21** (1976).
16. M. Borri and T. Merlini, A large displacement formulation for anisotropic beam analysis, *Meccanica* **21** (1986).
17. D.A. Danielson and D.H. Hodges, Nonlinear beam kinematics by decomposition of the rotation tensor, *ASME Journal of Applied Mechanics* **55** (1987).
18. C.E.S. Cesnik and D.H. Hodges, VABS: A new concept for composite rotor blade cross-sectional modeling, *Journal of the American Helicopter Society* **42** (1) (1997).